

Resonance Raman Characterization of Proteorhodopsin's Chromophore Environment

Richard A. Krebs, David Dunmire, Ranga Partha, and Mark S. Braiman*

Syracuse University Chemistry Department, Syracuse, New York 13244-4100

Received: March 5, 2003

Proteorhodopsin (pR) is a bacteriorhodopsin (bR) homologue, recently discovered in oceanic bacterioplankton, which functions as a light-driven proton pump. Resonance Raman spectra of pR excited with 532-nm light indicate that there are two subpopulations of pR within the sample solubilized in octylglucoside detergent and maintained in a light-adapted state in a spinning Raman cell. The subpopulations exhibit two distinct chromophore environments, as evidenced by two sets of split peaks, 1642/1655 cm^{-1} (corresponding to the Schiff base $\nu_{\text{C=N}}$ vibration) and 1244/1252 cm^{-1} (corresponding to a retinylidene-lysine N-C-H rock). These populations most likely arise either from different post-translational modifications of the heterologously expressed protein or from a mixture of retinal isomers (all-trans and 13-cis) that was previously reported to be present in light-adapted pR in a 60:40 ratio. However, the latter possibility seems at odds with the resonance Raman fingerprint spectral patterns in both natural-abundance and $15\text{-}^2\text{H}$ -retinal-substituted pR, which are consistent with an all-trans chromophore configuration similar to that of light-adapted bR.

Introduction

Proteorhodopsin (pR) is a 249-amino acid protein found in several uncultured species of γ -proteobacteria. When cloned and expressed in *Escherichia coli*, pR binds retinal and carries out light-activated proton pumping.^{1–3} Understanding the mechanism of pR could be of some importance to energy resources, since it is estimated to transduce solar energy into biochemical energy at a worldwide rate exceeding 1 TW ($\sim 10^{12}$ W), that is, at a substantial fraction of the rate of worldwide human energy consumption.

Like bacteriorhodopsin (bR), pR is a heptahelical integral membrane protein that binds retinal and contains many of the residues conserved among bR and related archaeal rhodopsin H^+ -pumps.¹ In fact, the overall homology between bR and pR in the retinal binding pocket is quite high, with two thirds of the residues being identical (Figure 1). In particular, homologues of arginine 82, aspartic acids 85, 96, and 212, and lysine 216 of bR are present in pR. In bR, lys-216 (conserved in pR as lys-231) binds retinal via a protonated Schiff's base linkage,^{1,4} while asp-212, asp-85, and arg-82 (conserved in pR as asp-227, asp-97, and arg-94) act in concert with other residues and water molecules as a complex counterion to the protonated Schiff base.^{5–7}

Further supporting links between the structure and function of bR and pR, flash photolysis experiments on pR in membrane vesicles at pH 7–10^{1,2,8,9} show evidence of transient photoproducts similar to the M ($\lambda_{\text{max}} \approx 410$ nm) and O ($\lambda_{\text{max}} \approx 610$ nm) intermediates of the bR photocycle. However, other experiments with pR in short-chain phospholipid at pH 9.5³ indicate the presence of M-like and N-like intermediates instead.

Dioumaev et al.⁸ recently reported Raman spectra of the unphotolyzed state of pR, using an excitation wavelength of 1064 nm. A disadvantage of using this excitation wavelength is the weak preresonant enhancement that it provides for the

Schiff base C=N stretch vibration near 1650 cm^{-1} ($\nu_{\text{C=N}}$), relative to overlapping Raman bands from water and from the abundant amide I modes of the protein. Resonance Raman (RR) spectroscopy using visible excitation wavelengths is generally a more useful tool for studying retinal proteins, since the chromophore can be more selectively excited, greatly reducing the relative size of Raman bands from the rest of the protein. This selectivity is of particular value in studying the pR chromophore environment because an acceptable signal-to-noise ratio can be obtained on partially purified samples.

RR has been used previously to elucidate the chromophore structure in the light-adapted and dark-adapted resting states of both bacteriorhodopsin (bR) and halorhodopsin (hR), as well as in their various photointermediates.^{10–17} Resonance Raman has been particularly important for showing the chromophore's protonation and hydrogen-bonding state and the cis–trans configuration of the C₁₃–C₁₄ double bond in each photoproduct. There are also a number of significant changes in its RR spectra observed during the acid-induced purple-to-blue transition of the unphotolyzed bR state.¹⁸

Here we show that the “red-to-purple” transition in pR, which is analogous to the purple-to-blue transition of bR, surprisingly does not produce similar changes in the RR spectrum. Furthermore, unlike light-adapted bR, light-adapted pR exhibits a heterogeneity in the $\nu_{\text{C=N}}$ frequency of its chromophore, as evidenced by a doublet $\nu_{\text{C=N}}$ RR band near 1648 cm^{-1} . The two components of this band might correspond to two molecular-weight variants seen in *E. coli*-expressed pR ($\sim 36\,000$ and $36\,500$ MW) that presumably differ only in their post-translational modifications.³

The splitting in the $\nu_{\text{C=N}}$ resonance Raman band is in any case indicative of two pR unphotolyzed states that exist in roughly equal proportions, something not observed under normal conditions in bR. This heterogeneity has implications for the efficiency of pR as an energy transducing protein. For laboratory investigations into the pR mechanism, the heterogeneity also indicates that it may be impossible to synchronously excite the

* Corresponding author. E-mail: mbraiman@syr.edu. Telephone: (315) 443-4691. Fax: (315) 443-4070.

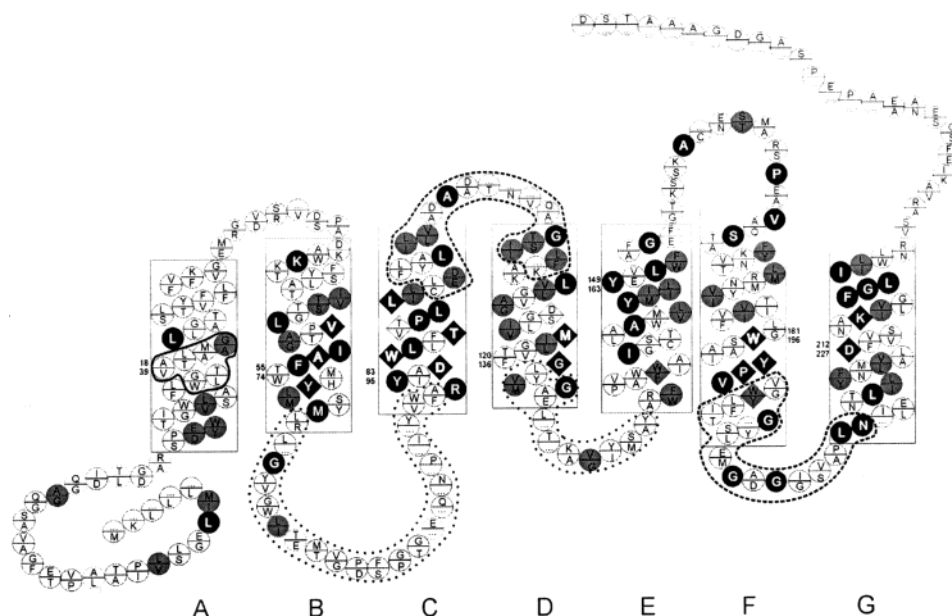


Figure 1. Primary sequence comparison between bR and pR, showing our proposed structural alignment. Each of the seven transmembrane helical regions (A–F) is indicated by a rectangle, with boundaries obtained by examining several of the high-resolution X-ray crystal structures of bR in the Protein Data Bank (1AP9, 1C3W). A circle or diamond enclosing only one letter corresponds to a sequence identity between pR (accession # AAG10475) and bR (gi 114811). In a split circle or diamond, the bR residue is on top and the pR residue that most likely fits into a similar position within the 3-D structure is given below. A diamond (◆) is used to indicate each residue that constitutes part of the retinal binding pocket. The sequence alignment (except for the five regions enclosed by curves) came from performing a standard protein BLAST search on pR and then displaying its simultaneous alignment with the entire bR superfamily (COG5524.1), including *H. salinarum* bR as a representative sequence. This was the only procedure that we found to give statistically significant alignment simultaneously over all seven helices. However, it results in several gaps of three or more residues in extracellular loops, extending in several cases to within the transmembrane helices. It was possible to reduce the number and size of the gaps in the B–C and D–E loop regions (inside the dotted curves) to a minimum, simply by taking the alignment within these regions from the alternative superfamily comparison to PFAM01036.6 (a subset of COG5524.1 containing only sequences from archaea). Large gaps in the C–D and F–G loop regions (inside the dashed curves) could be minimized only by performing a pairwise BLAST alignment using pR as the query sequence and bR as the target and selecting a gap opening penalty of 10 and extension penalty of 2. Several remaining compensated gaps in both opposing sequences, all within the short region enclosed by a solid curve, were eliminated without direct support from any BLAST alignment. However, this manual correction is justified by the unlikelihood of any disruption in secondary structure at the center of helix A.

H⁺-pumping photocycle without observing significant nonproductive photoreactions, even under conditions of complete light-adaptation.

Materials and Methods

Sample Preparation. Phenylsepharose-column-purified pR was obtained as previously described.³ During the chromophore regeneration step either natural-isotope-abundance retinal (Sigma) or the 15-²H-retinal derivative was added. The 15-²H-retinal was prepared by a previously published method involving reduction of *all-trans*-retinoic acid (Fisher) to retinal with LiAlH₄ (Sigma), followed by oxidation with activated MnO₂ (Aldrich) to retinal.¹⁵

The resulting pink-colored *E. coli* membranes containing pR were lysed and washed in a cholate solution; then the membranes were extracted with octyl-β-D-glucoside and applied to a Phenylsepharose column as described.³ Fractions with A₂₈₀/A₅₄₆ < 6 were pooled and then concentrated with Vivaspins (Vivascience, Hanover, Germany) concentrators to a volume of ~0.5 mL (A₅₄₆ ~ 5–8). Adjustment of the pH was accomplished by washing three times in Vivaspins concentrators with 100 mM HEPES containing 1% (w/v) octyl-β-D-glucoside (OG) at the selected pH. Exchange of deuterated buffer was accomplished by washing the sample two times with 20 volumes of the deuterated buffer using the Vivaspins concentrators.

Preparation of the control bR sample involved solubilizing purple membranes in a 0.5% OG solution [100 mM Na-HEPES, pH 7.1 (0.5 mL)] and then centrifuging (30 min, 9800g, 4 °C).

Spectroscopy. Raman spectra were measured with the samples in a quartz cell on a Spex spinning support, 1 cm radius, at 1680 rpm. The 532-nm excitation laser was a continuous-wave frequency-doubled Nd³⁺:YVO₄ laser (Spectra-Physics Millennia IIs Series). Right-angle-scattered emissions were focused through a Kaiser F/1.4 Holospec spectrograph, slit width 25 μm. The dispersed light was then focused onto a CCD detector (Princeton Instruments, model LN/CCD-1100PB/VISAR with a ST-130 controller). The resulting spectral resolution was 6 cm⁻¹.

Data were collected and analyzed by using Winspec, Grams/32, and Axum software. Baseline corrections were performed by multipoint baseline smoothing in the Grams/32 software. This software was also used for the peak fitting calculations. All spectra were normalized to the amplitude of the 1007 cm⁻¹ vibration in bR.

Results

Bacteriorhodopsin/Proteorhodopsin Comparisons. The RR spectra of bR and pR (Figure 2A and B) closely resemble each other. This is expected, given the high degree of conservation among the residues surrounding the retinal chromophore. However, there are some interesting differences. The most noticeable is the upshift and splitting of the bR 1639 cm⁻¹ peak to a doublet peak at 1642/1655 cm⁻¹ in pR (see Figure 2A and B as well as the expansion in Figure 3). The intensity maxima of the composite peaks of this doublet were determined by peak fitting to be at 1642 and 1655 cm⁻¹, and their relative integrated

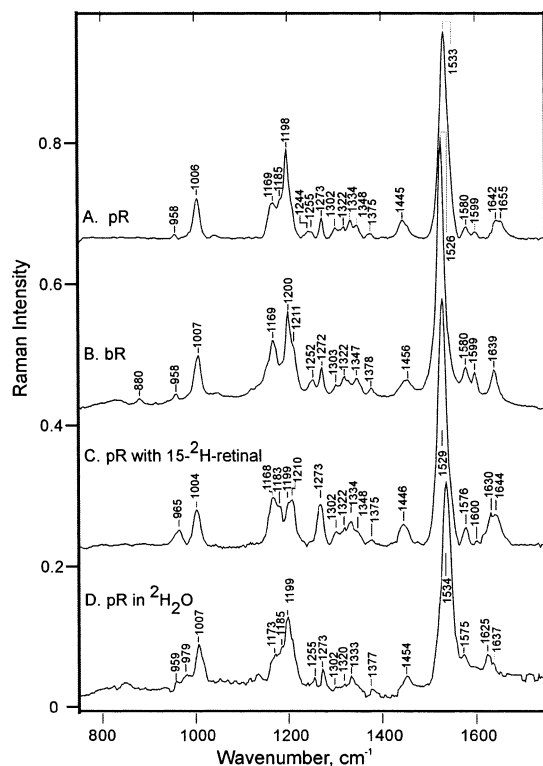


Figure 2. Comparison of 532-nm-excited resonance Raman spectra of bR and pR: (A) pR containing a retinal chromophore having natural isotope abundance and solubilized in normal (undeuterated) buffer containing 1.0% octylglucoside; (B) a similar bR sample, but in 0.5% octylglucoside; (C) a sample of pR as in part A, but containing 15- ^2H -retinal; (D) is a sample of pR as in part A, but in deuterated ($^2\text{H}_2\text{O}$) buffer. All measurements represent right-angle Raman scattering using a Spex quartz spinning cell and a CCD detector.

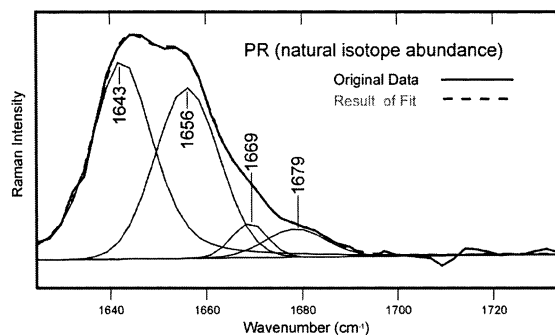


Figure 3. Curve fitting of the Schiff base stretching vibration spectral region in pR at pH 7.1 (from the same data as in Figure 2A). The two largest fitted peaks are centered at 1642 and 1656 cm^{-1} and have a 1:1 area ratio. The two smaller peaks centered at 1669 and 1679 cm^{-1} represent $\sim 10\%$ of the total peak area. Four mixed Gaussian/Lorentzian peaks (four optimized parameters each, i.e., area, center frequency, width, and percent Gaussian) plus a linear baseline (two parameters) were fitted to the original 46 data points in this spectral region.

intensities are in a ratio of 1:1 (Figure 3). The presence of a doublet was clearly confirmed in spectra of pR with 15- ^2H -retinal (Figure 2C and expansion in Figure 4).

Another significant difference between bR and pR was observed in the positions and relative intensities of several ethylenic stretching ($\nu_{\text{C}=\text{C}}$) vibrations. There is also a shift of the strongest ethylenic stretch band from 1526 cm^{-1} in bR to 1533 cm^{-1} in pR. This is consistent with the visible absorption maximum of pR at pH 7 (~ 545 nm, as opposed to ~ 570 nm for bR) and the well-known correlation between λ_{max} and the $\nu_{\text{C}=\text{C}}$ ethylenic stretch in retinal-protein complexes.¹⁹ Addition-

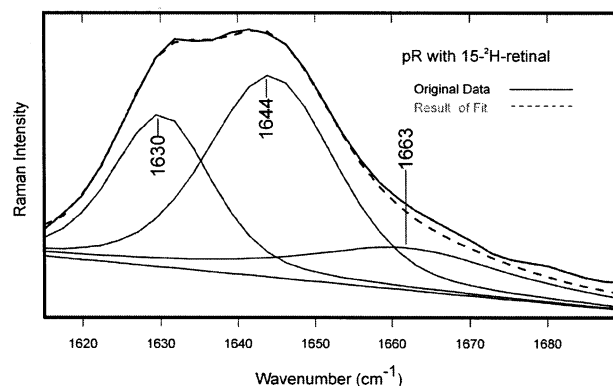


Figure 4. Curve fitting of the Schiff base region of the resonance Raman spectrum from pR containing 15- ^2H -retinal. The two fitted peaks are centered at 1630 and 1644 cm^{-1} and are in a 1.7:1 area ratio. Five mixed Gaussian/Lorentzian peaks plus a linear baseline were fitted to the original 32 data points in this spectral region.

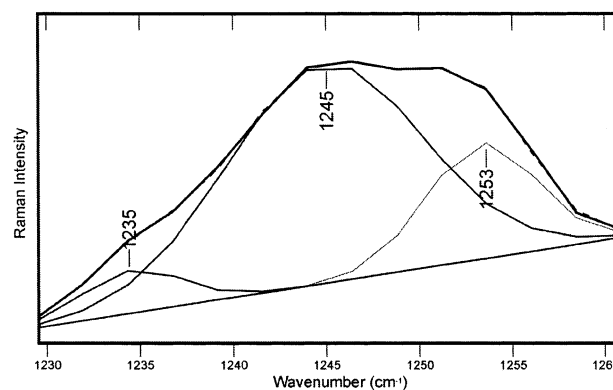


Figure 5. Curve fitting of the lysine methylene rock region of pR. The two largest fitted peaks are centered at 1245 and 1253 cm^{-1} and have a 4:1 area ratio. The third peak, centered at 1235 cm^{-1} , represents about 7% of the total peak area. Three mixed Gaussian/Lorentzian peaks (four parameters each) plus a linear baseline (two parameters) were fitted to the original 14 data points in this spectral region, significantly reducing the statistical significance of any of the fitted parameters relative to the fits in Figures 3 and 4.

ally, the pR peak corresponding to the 1599 cm^{-1} $\nu_{\text{C}=\text{C}}$ vibration in bR has about 60% of the intensity of the bR band.

The region between 1500 and 1250 cm^{-1} is generally quite similar for bR and pR, showing only a few clear differences. The most important is that the lysine ϵ -methylene rock, which was previously assigned at 1252 cm^{-1} in the bR spectrum,²⁰ appears as a clear doublet in the pR spectrum (Figure 2B). The fitted positions of the component bands are 1252 and 1242 cm^{-1} , with an additional minor component at 1235 cm^{-1} . These three fitted bands have relative intensities of 3:10:1 (Figure 5). In addition, there is an apparent upshift of the 1322 cm^{-1} bR peak (previously assigned as due to C_7H and C_8H rock vibrations²⁰ to 1334 cm^{-1} in pR, and a frequency shift in the 1456 cm^{-1} bR band to 1445 cm^{-1} in pR is apparent.

The only apparent differences between pR and bR in the rest of the fingerprint C—C stretch region (1100–1250 cm^{-1}) are intensity changes: pR shows a decrease in the ~ 1211 cm^{-1} shoulder on the 1200 cm^{-1} peak and increases in the bands at ~ 1200 and ~ 1185 cm^{-1} .

Below 1100 cm^{-1} , there are no significant frequency shifts observed between pR and light-adapted bR. However, it is noteworthy that several broad, weak bands between 750 and 950 cm^{-1} in the resonance Raman spectrum of light-adapted bR are not even clearly observable in the pR spectrum.

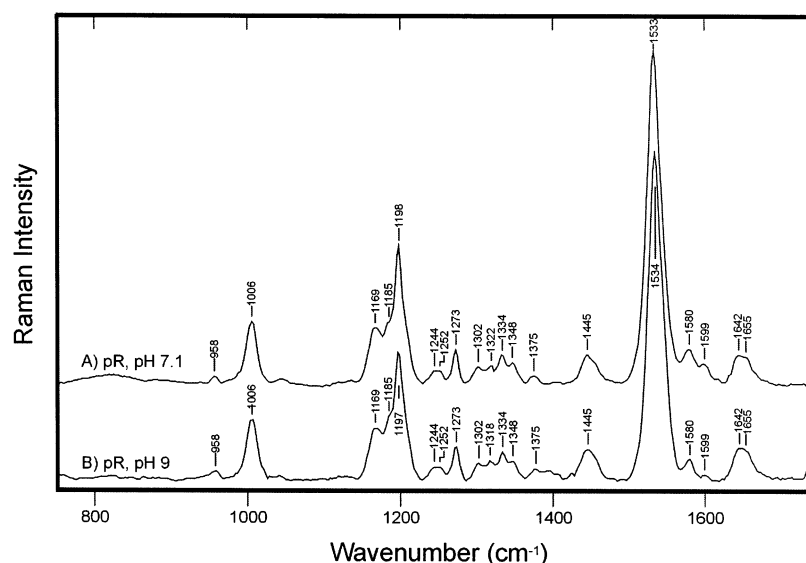


Figure 6. Comparison of resonance Raman spectra of pR at pH values of (A) 7.1 and (B) 9. Spectra were measured as in Figure 2. However, the data at pH 9 were from a more dilute sample and required some smoothing (five-point Savitzky–Golay procedure) to be presented in this figure; therefore, the same smoothing was applied to the data at pH 7.1, resulting in slightly lower resolution than that for the original data in Figure 2.

Deuteration at C₁₅. Reconstitution of pR with 15-²H-retinal gave a RR spectrum that is also very similar to that previously measured on 15-²H-retinal-reconstituted bR.^{11,16,17} The most obvious isotope-induced frequency shift is that of the 1642/1655 cm⁻¹ doublet band, which downshifts to give bands centered at 1630/1644 cm⁻¹ (Figure 2A and C). Peak fitting of this region gives relative intensities of 1:1.7 for the component peaks at 1630 and 1644 cm⁻¹ (Figure 4). The downshifts of both components are similar in magnitude to the 10-cm⁻¹ shift of $\nu_{C=N}$ (from 1640 to 1630 cm⁻¹) induced by C₁₅-deuteration in bR.¹⁶

The strongest $\nu_{C=C}$ band downshifts to 1529 cm⁻¹. The 1599 cm⁻¹ peak that showed a lower intensity in the ¹H-15-retinal pR loses further intensity upon deuteration. There is a decrease in intensity of the 1199 cm⁻¹ band and emergence of a 1210 cm⁻¹ band. The appearance of the 1210 cm⁻¹ band in the ²H-15-retinal bR spectrum could be due to an underlying peak already present in the ¹H-15-retinal pR spectrum becoming visible with the intensity decrease of 1198 cm⁻¹.

The 1244/1252 cm⁻¹ doublet peak present in undeuterated pR (Figure 2A, 5) disappears upon C₁₅-deuteration (Figure 2C), as observed previously for the 1255-cm⁻¹ band in bR. There is a substantial loss of intensity in both the 1200 and 1252 cm⁻¹ lines in light-adapted bR when C₁₅-H is deuterated. This band was assigned to a C–H rock of Lys-216 in bR (Lys-231 in pR). Upon C₁₅-deuteration, it is calculated to downshift under the 1200 cm⁻¹ band due to its coupling to the Schiff base linkage. Also, there is a shift of intensity to 958 cm⁻¹ which is the C₁₅-D in-plane bend vibration.

In bR containing 15-²H-retinal, a downshift of 9 cm⁻¹ was observed in the 1639 cm⁻¹ band, as well as a small (4 cm⁻¹) decrease in frequency of the main ethylenic stretch band from 1526 to 1522 cm⁻¹. There appear to be no significant changes in the intensity of the 1526 cm⁻¹ band between ¹H-15- and ²H-15-retinal bR in previously published data.^{16,17} This result differs from the ~35% relative intensity increase observed in the analogous pR peak (compare Figure 2A and C).

Another small difference between pR and bR upon C₁₅-deuteration is that pR containing 15-²H-retinal (Figure 2C) apparently lacks an analogue of the clear 785 cm⁻¹ peak in ²H-15-retinal bR which was assigned to the C₁₅-DOOP (deuterium

out-of-plane) wag.²⁰ We do observe a significant increase in the intensity of the 958 cm⁻¹ band as well as a slight increase in frequency (965 cm⁻¹).

Deuteration at the Schiff Base Nitrogen. Solubilization of pR in deuterated buffer elicited a distinct set of vibrational changes (Figure 2A and D). As with C₁₅-deuteration, most of these are similar to those observed in previous comparable bR experiments.^{20,21} The Schiff base $\nu_{C=N}$ bands (1642/1655 cm⁻¹) downshift and coalesce into a single peak at 1627 cm⁻¹. Other changes in the pR spectrum upon ²H₂O exchange that are analogous to those seen previously in bR²¹ include the downshift of the N–D in-plane rock from near 1350 cm⁻¹ to 979 cm⁻¹ (977 cm⁻¹ in bR), resulting in intensity shifts due to changes in vibrational mixing with other bands in the 1300–1400 cm⁻¹ region, and in particular leading to a prominent peak at 1355 cm⁻¹, as well as a downshifted $\nu_{C=C}$ band (from 1580 to 1575 cm⁻¹). In addition, we observe the coalescence and upshift of the doublet bands assigned to the pR lysine N–C–H rock from 1244 and 1252 to 1255 cm⁻¹. The latter is similar to the frequency observed for this vibration in deuterium-exchanged bR.

Effects of the Red-to-Purple Transition on the Resonance Raman Spectrum of pR. Bacteriorhodopsin has been shown to have titratable residues in the retinal pocket that can shift the visible absorption band of the protein. Specifically, asp-85 can be protonated below pH 2.5, causing a shift of the chromophore absorption maximum from that associated with a purple color, bR₅₆₈, to the “blue” form of bR, bR₆₀₅.^{18,22} The pK_a of this purple-to-blue transition in bR is 2.5–2.8.²³

A similar titration of the homologous Schiff base counterion residue (asp-97) in pR occurs with a pK_a between 7.1 and 8.2, depending on measurement conditions,^{8,9} and has been designated the “red-to-purple” transition.²⁴ Since pR undergoes a substantial λ_{\max} shift from ~521 to 544 nm^{8,24} during this transition, the RR spectrum would be expected to change as well. However, raising the pH of the pR solution through the pK_a of the red-to-purple transition, previously measured as ~8.2 for pR in OG solution,²⁴ brought about no clear Raman spectral shifts (Figure 6). This is somewhat surprising. Given the λ_{\max} shift observed over this pH range, perturbation of many more Raman frequencies might be expected. In particular, it is

surprising that the $\nu_{\text{C=N}}$ frequencies/band shapes do not change significantly during the red-to-purple transition.

It is important to note that, regardless of pH, no significant peaks below 950 cm^{-1} appear in the pR spectrum, in particular no peak near 800 cm^{-1} . This was different from the case with bR where the RR spectrum of the low-pH (blue) form shows a strong C—H out-of-plane wag near 800 cm^{-1} , indicating significant formation of the 13-cis, 15-syn form of the chromophore present in dark-adapted bR.¹⁸

Discussion

Overall, either C_{15} -deuteration or N-deuteration of the retinylidene Schiff base in pR causes remarkably similar changes to those observed previously in analogous bR isotope-labeling experiments. On the basis of this, we conclude that the retinal binding pockets of pR and bR are generally similar, with the important exception of an increased Schiff base H-bond strength in pR. These conclusions agree with those of previous workers who obtained preresonance Raman spectra of pR (without isotope labeling) using near-infrared excitation.⁸

Besides vibrations from the protonated Schiff base moiety, there are only minor differences between pR and bR in several of the peaks corresponding to the central region of the conjugated ethylenic chain, in particular in several fingerprint C—C stretch bands ($1100\text{--}1250\text{ cm}^{-1}$), the methyl group vibrations near 1450 cm^{-1} , a C=C stretch band at 1599 cm^{-1} , and the 1184 cm^{-1} band. These differences may presumably be related to environmental changes in the retinal binding pocket along the polyene chain and β -ionone ring.

A homology comparison is provided (Figure 1) that relates the amino acid side chains in the retinal binding pocket of pR and bR. Of the 21 residues that constitute the retinal binding pocket, as defined by Khorana²⁵ and Henderson et al.,²⁶ there are only 7 nonidentities between bR and pR (Met \rightarrow Ala in helix A; Thr \rightarrow Val in helix C; Asp \rightarrow Ser in helix D; Met \rightarrow Trp, Ser \rightarrow Gly, and Trp \rightarrow Phe in helix E; and Trp \rightarrow Tyr in helix F). A majority of these changes are adjacent to the β -ionone ring or the $\text{C}_6\text{--C}_{10}$ portion of the ethylenic chain, and they might easily give rise to some of the minor spectral changes observed between bR and pR.

Increased H-Bonding Strength of the Schiff Base and Its Counterion. None of the amino acid substitutions indicated in Figure 1 can be directly associated with the large upshift observed for the $\nu_{\text{C=N}}$ band of pR, in comparison to bR. It has been shown previously^{27–30} that the interaction between the Schiff base and its counterion strongly affects the delocalization of the positive charge in the retinylidene chromophore. The Schiff base counterion has been described as a complex consisting of Arg-82, Asp-85, Trp-86, Asp-212, and Tyr-185 which carries a net negative charge.²⁶ This, in turn, affects the frequency of the stretch vibrations coupled to the affected bonds and the λ_{max} of the protein as a whole.

A weaker Schiff base/counterion H-bonding interaction is directly associated with a downshift of the chromophore's $\nu_{\text{C=N}}$ frequency and, more indirectly, with a downshift in $\nu_{\text{C=C}}$ and a red shift in the visible λ_{max} due to a greater degree of charge delocalization along the conjugated π -electron system.^{27,28–31} In pR, the $\nu_{\text{C=C}}$ stretch frequencies are upshifted and the visible λ_{max} is blue-shifted relative to the case of bR.^{3,32} Therefore, in accordance with theory developed by other workers,^{20,33} we conclude that pR has a stronger Schiff base/counterion hydrogen bonding interaction than bR.

This in turn is consistent with our group's conclusion that there is a weakened interaction between Arg-94 and Asp-97 in

pR. This conclusion was based in large measure on our observation that Arg-94 mutation has little effect on the Asp-97 pK_a .²⁴ It was concluded that Arg-94 in pR is likely to be shifted toward the extracellular space, away from the retinal chromophore, as occurs in sensory rhodopsin II from *Natronobacterium pharaonis* (NpsR-II).³⁴ Removal of the guanidinyll positive charge from the complex counterion would also be expected to lead to a stronger H-bonding interaction and therefore an upshift of the $\nu_{\text{C=N}}$ frequency. Our resonance Raman results—in particular, the similar $\nu_{\text{C=N}}$ frequencies of sR-II (1645 cm^{-1} (ref 35)) and pR ($1642/1655\text{ cm}^{-1}$, Figure 2A)—thus provide additional support for the conclusion that pR has an Arg-94 position similar to that in NpsR-II and unlike that in bR.

Structural Heterogeneity in the Schiff Base Environment.

Our pR RR spectra consistently show the Schiff base $\nu_{\text{C=N}}$ band to be a doublet consisting of two barely resolved bands. The fitted band shapes are considerably broader than our measurement resolution of 6 cm^{-1} . Therefore, the observed near-merging of these bands is due to their inhomogeneously broadened band shape rather than insufficient instrumental resolution. In fact, no splitting of the $\nu_{\text{C=N}}$ Raman band of pR was noted in previous measurements⁸ despite their better spectral resolution. The inability to detect the splitting in this earlier work was likely related to the choice of Raman excitation wavelength. A 1064-nm Raman excitation wavelength does not resonantly enhance the Schiff base vibration, relative to other Raman bands from pR and from solvent, nearly as well as the 532 nm excitation wavelength that we used. The preresonant Raman spectrum of pR measured with 1064-nm light therefore has substantial water (H—O—H bend) and amide I (protein backbone) band intensities near 1650 cm^{-1} that interfere with accurate measurement of the $\nu_{\text{C=N}}$ band shape.

Our resonance Raman spectrum of pR containing C_{15} -deuterated retinal precludes that the 1655 cm^{-1} component of this split band could arise from H_2O -bending or amide I vibrations, since this component clearly downshifts upon substitution of the nonexchangeable $\text{C}_{15}\text{--H}$. In fact, it is most likely that both 1642 and 1655 cm^{-1} components downshift by $\sim 11\text{ cm}^{-1}$. There is a possible alternative assignment for the $\nu_{\text{C=N}}$ bands in unsubstituted and $15\text{-}^2\text{H}$ -retinal-reconstituted samples, namely, that the $\nu_{\text{C=N}}$ band is a singlet at 1655 cm^{-1} and this band shifts down to 1630 cm^{-1} upon C_{15} -deuteration. This would leave an unidentified intense $\sim 1645\text{ cm}^{-1}$ band at nearly the same position in both undeuterated and C_{15} -deuterated spectra.

This set of assignments is unlikely on several counts. First, it posits a very large (25-cm^{-1}) shift of the $\nu_{\text{C=N}}$ stretch upon deuteration at C_{15} . This would be unprecedented among the archaeal rhodopsins, in which no examples have ever been demonstrated of a C_{15} -deuteration downshift of greater than 17 cm^{-1} , observed for bR in the M state.¹⁶ More problematic, however, is that there is no good explanation for having a resonantly enhanced vibration at 1645 cm^{-1} that is insensitive to C_{15} -deuteration. Furthermore, this explanation is inconsistent with the observation that other vibrational bands associated with the Schiff base group are also observed to be split in pR, for example, the N—C—H rock vibration of Lys-231. In bR, this N—C—H rock vibration appears as a singlet at 1252 cm^{-1} (ref 20). In pR, however, this band also splits into a doublet ($1244/1252\text{ cm}^{-1}$). Likewise, the Schiff base C—NH rock is assigned in the bR Raman spectrum as a single band at 1348 cm^{-1} (ref 20) but appears to upshift and broaden in pR, once again

indicating a stronger H-bond and a heterogeneous environment for the Schiff base group.

A downshift of the $1642/1655\text{ cm}^{-1}$ $\nu_{\text{C=N}}$ doublet was also expected upon exchanging a deuteron for a proton on the Schiff base. Instead of a downshifted doublet, however, only a single band is observed in the N-deuterated Raman spectrum of pR (Figure 2D). The coalescence of the doublet is possibly due to a lessened sensitivity of $\nu_{\text{C=N}}$ to the two different types of H-bonding environment that are present in pR samples, once the C=N–H bend downshifts from near 1350 cm^{-1} to below 1000 cm^{-1} upon deuteration. A similar effect was observed for halorhodopsin in the presence of nitrate ion; in $^1\text{H}_2\text{O}$, a $\nu_{\text{C=N}}$ doublet was observed, whereas in $^2\text{H}_2\text{O}$ only one $\nu_{\text{C=N}}$ band was seen.³⁶ A related effect is presumed to lead to the coalesced 1255 cm^{-1} band (due to the N–C–H rock of Lys-231, which is presumably coupled to the C=N–H bend) in the deuterium-exchanged pR sample (Figure 2D).

Possible Sources of pR Sample Heterogeneity. The most likely explanation for the splitting of the $\nu_{\text{C=N}}$ Raman band of pR, as well as the lys-231 rock vibration near 1250 cm^{-1} , is that, under our measurement conditions, pR has a heterogeneous structure near the Schiff base portion of the retinal chromophore, involving a local H-bonding perturbation. However, this could be caused by a number of underlying phenomena.

One possibility that we addressed experimentally was that the two $\nu_{\text{C=N}}$ bands at pH 7 arose from a mixture of the high-pH (red) and low-pH (purple) forms of the protein, since the pH spectrum was measured only ~ 1 pH unit below the pK_a for the red-to-purple transition. However, this possibility is now ruled out, since the relative intensities of the 1642 and 1655 cm^{-1} bands do not change between pH 7 and 9 (Figure 6).

There appear to be three remaining possibilities for the observed $\nu_{\text{C=N}}$ Raman band-splitting in pR. First, some type of reversible ligand binding, similar to that seen for nitrate ions in halorhodopsin (hR), might conceivably cause two distinct populations of Schiff base chromophore to be present in the unphotolyzed state of pR.^{36,37} However, our sample solutions lacked small anions (i.e. with a Stokes radius $< 1.65\text{ \AA}$).³⁸ We used only Na^+ and HEPES in our samples, with all other ion concentrations below 1 mM . Specific binding of Na^+ or HEPES is unlikely to be the cause of the $\nu_{\text{C=N}}$ Raman band-splitting in pR, but it remains conceivable that nonspecific ion binding could be involved. Unfortunately, pR is not very stable at low ionic strengths. Therefore, only an examination of RR spectra using many other buffer conditions will allow ruling out this possibility.

A second possibility is that the split $\nu_{\text{C=N}}$ band in the pR resonance Raman spectrum is directly related to the doublet band observed for purified pR on SDS–polyacrylamide gel electrophoresis.³ From that result, it is clear that pR exists in two stable variants, at least when purified from the *E. coli* expression system. Since only one pR gene was introduced into this heterologous expression system, these two variants presumably differ in their post-translational modifications, by nearly 500 Da of apparent molecular weight.³ These different (but unknown) post-translational modifications might correspond to two populations of pR with different conformations. These could constrain the chromophore counterion residues (presumably including Arg-94) to adopt two different sets of positions. This would result in two distinct sets of H-bonding interaction strengths with the protonated Schiff base group and lead to the observed band splitting. This possibility must eventually be tested by finding a way to eliminate the production of one of the two molecular-weight variants of pR, or else to separate

them. It is unfortunately not as simple as cutting apart the bands on the gel and eluting, since the SDS present during electrophoresis denatures pR (irreversibly, so far as we yet know).

Finally, it is possible that the pR resonance spectra we obtained represent two interconvertible photointermediates: for example, the unphotolyzed state and some photoproduct with a lifetime long in comparison to the rotational period of the Raman cell. If the lifetime were not too long, however, we might expect to be able to change the relative amounts of the two species by varying pR concentration, laser power, spinning speed, and so forth. There was no indication of multiple species observed when the laser power or sample spinning speed was changed by a factor of 2–3 (data not shown). Therefore, any photoproduct state involved in producing the doublet band would be expected to have a quite long lifetime.

It is unlikely that this long-lived state could correspond to any of the known bR photoproducts. One of the most distinctive peaks for bR photointermediates K through N is the 13-*cis*-retinal peak near 800 cm^{-1} (refs 15–17). Neither our group nor Dioumaev et al.⁸ observe evidence of such a band that would indicate 13-*cis* chromophore, certainly not enough to account for the $\sim 50\%$ occupancy indicated by the nearly equal bands at $1642/1655\text{ cm}^{-1}$.

Dioumaev et al.⁸ reported the existence of seven transient states, the last of which have decay times of 35 and 230 ms. Their time-resolved FTIR of photolyzed pR protein measured between these longest two decay times showed evidence of a chromophore that was protonated and in the all-*trans* conformation, but distorted, similar to the chromophore of O-state bR. The long-lived nature of this intermediate makes it possible that it builds up to a detectable concentration in our Raman samples. However, such an O-like intermediate would be expected to show additional chromophore vibrations in known spectral regions, for example, at 1509 cm^{-1} (17 cm^{-1} downshift of the ethylenic stretch), 978, and 945 cm^{-1} (ref 17). No such peaks are observed in our pR spectrum. This indicates that while some O-like pR may be present, it is not at a concentration sufficient to account for the nearly equal intensity Schiff base Raman bands that we observe.

We conclude that our pR Raman sample heterogeneity cannot be due to a photoproduct analogous to any from the bR photocycle. Nevertheless, it has recently been reported⁹ that light-adapted pR contains a substantial amount (40%) of a 13-*cis*-retinal-containing species, which decays with a 12-min lifetime. The identity of this unusual 13-*cis* component of light-adapted pR remains unclear; nor is it clear whether it could account for our observed $\nu_{\text{C=N}}$ band splitting. In particular, it must be very different from any of the known bR species that contain a 13-*cis* chromophore, since our data and those of others⁸ indicate that it must lack a RR band near 800 cm^{-1} and that it shows a fingerprint ($1100\text{--}1250\text{ cm}^{-1}$) spectral region that closely matches that of the all-*trans* component of light-adapted bR.

Conclusions

Resonance Raman spectra of pR excited with 532-nm light indicate that there are two subpopulations of pR within the sample solubilized in octylglucoside detergent and maintained in a light-adapted state in a spinning Raman cell. The two populations exhibit two distinct chromophore environments, as evidenced by two sets of split peaks, $1642/1655\text{ cm}^{-1}$ (corresponding to the $\nu_{\text{C=N}}$ Schiff base vibration) and $1244/1252\text{ cm}^{-1}$ (corresponding to a retinylidene–lysine N–C–H rock). These populations most likely arise from different post-translational

modifications of the *E. coli*-expressed protein. In the future, the exact nature of these modifications will have to be determined as well as whether the heterogeneity is present in the as-yet-uncultured native host of pR or it is an artifact due to heterologous expression.

A possible alternative explanation for the two distinct subpopulations that has not been ruled out is that the two distinct groups of Schiff base vibrations arise from a long-lived 13-cis photoproduct that was previously reported to be present in light-adapted pR at a level of 40%.⁹ However, this possibility seems at odds with the resonance Raman spectral fingerprint patterns in both isotope-substituted and unsubstituted pR. These are instead consistent with a chromophore configuration that is almost entirely, if not exclusively, all-trans.

Acknowledgment. This work was supported by Syracuse University. We thank Lawrence Nafie and Teresa Freedman for allowing us to use their Raman spectrometer for these measurements; Anne Marie DeVita as well as Robert Birge and his research group for helping with sample preparations, and Daniel Marenda for critical analysis of this manuscript.

References and Notes

- (1) Bějá, O.; Aravind, L.; Koonin, E. V.; Suzuki, M. T.; Hadd, A.; Nguyen, L. P.; Jovanovich, S. B.; Gates, C. M.; Feldman, R. A.; Spudich, J. L.; Spudich, E. N.; DeLong, E. F. *Science* **2000**, *289*, 1902–1906.
- (2) Bějá, O.; Spudich, E. N.; Spudich, J. L.; Leclerc, M.; DeLong, E. F. *Nature* **2001**, *411*, 786–789.
- (3) Krebs, R. A.; Alexiev, U.; Partha, R.; DeVita, A. M.; Braiman, M. S. *BMC Physiol.* **2002**, *2*, 5.
- (4) Rothschild, K. J.; Argade, P. V.; Earnest, T. N.; Huang, K.-S.; London, E.; Liao, M.-J.; Bayley, H.; Khorana, H. G.; Herzfeld, J. *J. Biol. Chem.* **1982**, *257*, 8592–8595.
- (5) Braiman, M. S.; Mogi, T.; Marti, T.; Stern, L. J.; Khorana, H. G.; Rothschild, K. J. *Biochemistry* **1988**, *27*, 8516–8520.
- (6) Stern, L. J.; Khorana, H. G. *J. Biol. Chem.* **1989**, *264*, 14202–14208.
- (7) de Groot, H. J. M.; Harbison, G. S.; Herzfeld, J.; Griffin, R. G. *Biochemistry* **1989**, *28*, 3346–3353.
- (8) Dioumaev, A. K.; Brown, L. S.; Shih, J.; Spudich, E. N.; Spudich, J. L.; Lanyi, J. K. *Biochemistry* **2002**, *41*, 5348–5358.
- (9) Freidrich, T.; Geibel, S.; Kalmbach, R.; Chizhov, I.; Ataka, K.; Heberle, J.; Engelhard, M.; Bamberg, E. *J. Mol. Biol.* **2002**, *321*, 821–838.
- (10) Ames, J. B.; Raap, J.; Lugtenburg, J.; Mathies, R. A. *Biochemistry* **1992**, *31*, 12546–12554.
- (11) Hildebrandt, P.; Stockburger, M. *Biochemistry* **1984**, *23*, 5539–5548.
- (12) Braiman, M. S.; Mathies, R. *Methods Enzymol.* **1982**, *88*, 648–659.
- (13) Stockburger, M.; Klusman, W.; Gattermann, H.; Massig, G.; Peters, R. *Biochemistry* **1979**, *18*, 4886–4900.
- (14) Terner, J.; Hsieh, C.-L.; Burns, A. R.; El-Sayed, M. A. *Proc. Natl. Acad. Sci. USA* **1979**, *76*, 3046–3050.
- (15) Braiman, M. S.; Mathies, R. A. *Proc. Natl. Acad. Sci. U.S.A.* **1982**, *79*, 403–407.
- (16) Braiman, M. S.; Mathies, R. *Biochemistry* **1980**, *19*, 5421–5428.
- (17) Smith, S. O.; Pardo, J. A.; Mulder, P. P. J.; Curry, B.; Lugtenburg, J.; Mathies, R. *Biochemistry* **1983**, *22*, 6141–6148.
- (18) Smith, S. O.; Mathies, R. A. *Biophys. J.* **1985**, *47*, 251–254.
- (19) Doukas, A. G.; Aton, B.; Callender, R. H.; Ebrey, T. G. *Biochemistry* **1978**, *17*, 2430–2435.
- (20) Smith, S. O.; Braiman, M. S.; Myers, A. B.; Pardo, J. A.; Courtin, J. M. L.; Winkel, C.; Lugtenburg, J.; Mathies, R. A. *J. Am. Chem. Soc.* **1987**, *109*, 3108–3125.
- (21) Smith, S. O.; Pardo, J. A.; Lugtenburg, J.; Mathies, R. A. *J. Phys. Chem.* **1987**, *91*, 804–819.
- (22) Metz, G.; Siebert, F.; Engelhard, M. *FEBS Lett.* **1992**, *303*, 237–241.
- (23) Balashov, S. P.; Govindjee, R.; Kono, M.; Imasheva, E.; Lukashev, E.; Ebrey, T. G.; Crouch, R. K.; Menick, D. R.; Feng, Y. *Biochemistry* **1993**, *32*, 10331–10343.
- (24) Partha, R.; Krebs, R. A.; Caterino, T. L.; Braiman, M. S. Submitted.
- (25) Khorana, H. G. *J. Biol. Chem.* **1988**, *263*, 7439–7442.
- (26) Henderson, R.; Baldwin, J. M.; Ceska, T. A.; Zemlin, F.; Beckmann, E.; Downing, K. H. *J. Mol. Biol.* **1990**, *213*, 899–929.
- (27) Bhat, P. E.; Mohler, J. H. *Biochemistry* **1975**, *14*, 2304–2309.
- (28) Harbison, G. S.; Herzfeld, J.; Griffin, R. G. *Biochemistry* **1983**, *22*, 1–5.
- (29) Lin, S. W.; Fodor, S. P. A.; Miercke, L. J. W.; Shand, R. F.; Betlach, M. C.; Stroud, R. M.; Mathies, R. A. *Photochem. Photobiol.* **1991**, *53*, 341–346.
- (30) Spudich, J. L.; McCain, D. A.; Nakanishi, K.; Okabe, M.; Shimizu, N.; Rodman, H.; Honig, B.; Bogomolni, R. A. *Biophys. J.* **1986**, *49*, 479–483.
- (31) Baasov, T.; Sheves, M. *J. Am. Chem. Soc.* **1985**, *107*, 7524–7533.
- (32) London, E.; Khorana, H. G. *J. Biol. Chem.* **1982**, *257*, 7003–7011.
- (33) Rodman-Gilson, H. S.; Honig, B. H.; Croteau, A.; Zarrilli, G.; Nakanishi, K. *Biophys. J.* **1988**, *53*, 261–269.
- (34) Ren, L.; Martin, C. H.; Wise, K. J.; Gillespie, N. B.; Luecke, H.; Lanyi, J. K.; Spudich, J. L.; Birge, R. R. *Biochemistry* **2001**, *40*, 13906–13914.
- (35) Gellini, C.; Lüttenberg, B.; Sydor, J.; Engelhard, M.; Hildebrandt, P. *FEBS Lett.* **2000**, *472*, 263–266.
- (36) Pande, C.; Lanyi, J. K.; Callender, R. H. *Biophys. J.* **1989**, *55*, 425–431.
- (37) Lanyi, J. K.; Duschl, A.; Varo, G.; Zimányi, L. *FEBS Lett.* **1990**, *265*, 1–6.
- (38) Schobert, B.; Lanyi, J. K. *Biochemistry* **1986**, *25*, 4163–4167.